Instabilities on the Dynamics of Inertial Particles

Themistoklis Sapsis & George Haller

Department of Mechanical Engineering

Massachusetts Institute of Technology

Applied Dynamics and Geometric Mechanics, Oberwolfach

July 20-26, 2008

Introduction

Finite-size or inertial particle dynamics in fluid flows can differ markedly from infinitesimal particle dynamics: both clustering and dispersion are well documented phenomena in inertial particle motion, while they are absent in the incompressible motion of infinitesimal particles. As we show, these peculiar asymptotic features are governed by a lower-dimensional inertial equation which is determined explicitly. Moreover, the limit of validity of the above equation is given explicitly through an analytical criterion that predicts the regions where dynamical instabilities on the motion of inertial particles will occur.

Let $\boldsymbol{u}(t, \boldsymbol{x})$ denote the velocity field of a two- or three-dimensional fluid flow of density ρ_f, with $\boldsymbol{x}$ referring to spatial locations and t denoting time. The fluid fills a compact (possibly time-varying) spatial region D with boundary ∂D; we assume that D is a uniformly bounded smooth manifold for all times. We also assume $\boldsymbol{u}(t, \boldsymbol{x})$ to be r times continuously differentiable in its arguments for some integer $r \geq 1$. We denote the material derivative of $\boldsymbol{u}$ by

$$\frac{D\boldsymbol{u}}{Dt} = \frac{\partial \boldsymbol{u}}{\partial t} + (\nabla \boldsymbol{u})\boldsymbol{u}$$

where ∇ denotes the gradient operator with respect $\boldsymbol{x}$. Let $\boldsymbol{x}(t)$ denote the path of a finite-size particle of density ρ_p immersed in the fluid. If the particle is spherical with sufficiently small radius, its velocity $\boldsymbol{v}(t)$ satisfies the equation of motion (cf. Maxey and Riley)

$$\dot{\boldsymbol{v}} - \frac{3R}{2}\frac{D\boldsymbol{u}}{Dt} = -\mu(\boldsymbol{v} - \boldsymbol{u}) + \left(1 - \frac{3R}{2}\right)\boldsymbol{g} \qquad (1)$$

With $R = 2\rho_f / (2\rho_f + \rho_p)$, $\mu = R / St$ where St is the Stokes number and t, v, u and g denote nondimensional variables. The density ratio R distinguishes neutrally buoyant particles ($R = 2/3$) from aerosols ($0 < R < 2/3$) and bubbles ($2/3 < R < 2$). The 3R/2 coefficient represents the added mass effect: an inertial particle brings into motion a certain amount of fluid that is proportional to half of its mass.

Here we consider finite-size particle motion in general unsteady velocity fields, extending Fenichel's geometric approach from time-independent to time-dependent vector fields. Such an extension has apparently not been considered before in dynamical systems theory, thus the present work should be of interest in other applications of singular perturbation theory where the governing equations are non-autonomous.

Singular perturbation formulation

The derivation of the equation of motion is only correct under the assumption $\mu >> 1$, which motivates us to introduce the small parameter $\varepsilon = 1/\mu << 1$, and rewrite the equation of motion (1) as a first-order system of differential equations

$$\begin{aligned} \dot{\boldsymbol{x}} &= \boldsymbol{v} \\ \varepsilon \dot{\boldsymbol{v}} &= \boldsymbol{u}(t, \boldsymbol{x}) - \boldsymbol{v} + \varepsilon \frac{3R}{2}\frac{D\boldsymbol{u}(t,\boldsymbol{x})}{Dt} + \varepsilon\left(1 - \frac{3R}{2}\right)\boldsymbol{g} \end{aligned} \qquad (2)$$

This formulation shows that x is a slow variable changing at $O(1)$ speeds, while the fast variable $\boldsymbol{v}$ varies at speeds of $O(1/\varepsilon)$. To transform the above singular perturbation problem to a regular perturbation problem, we select an arbitrary initial time t_0 and introduce the fast time τ by letting $\varepsilon\tau = t - t_0$. This type of rescaling is standard in singular perturbation theory with $t_0 = 0$. The new feature here is the introduction of a nonzero present time t_0 about which we introduce the new fast time τ. This trick enables us to extend existing singular perturbation techniques to unsteady flows. Denoting differentiation with respect to τ by prime, we rewrite

$$\begin{aligned} \boldsymbol{x}' &= \varepsilon \boldsymbol{v} \\ \varphi' &= \varepsilon \\ \boldsymbol{v}' &= \boldsymbol{u}(t, \boldsymbol{x}) - \boldsymbol{v} + \varepsilon \frac{3R}{2}\frac{D\boldsymbol{u}(t,\boldsymbol{x})}{Dt} + \varepsilon\left(1 - \frac{3R}{2}\right)\boldsymbol{g} \end{aligned} \qquad (3)$$

where $\varphi \equiv t_0 + \varepsilon\tau$ is a dummy variable that renders the above system of differential equations autonomous in the variables $(\boldsymbol{x},\varphi,\boldsymbol{v}) \in D \times \mathbb{R} \times \mathbb{R}^n$; here n is the dimension of the domain of definition D of the fluid flow ($n = 2$ for planar flows, and $n = 3$ for three-dimensional flows).

Slow manifold and inertial equation

The $\varepsilon = 0$ limit of system (3)

$$\begin{aligned} \boldsymbol{x}' &= 0 \\ \varphi' &= 0 \\ \boldsymbol{v}' &= \boldsymbol{u}(t, \boldsymbol{x}) - \boldsymbol{v} \end{aligned} \qquad (4)$$

has an $(n + 1)$-parameter family of fixed points satisfying $\boldsymbol{v} = \boldsymbol{u}(\boldsymbol{x},\varphi)$. More formally, for any time $T > 0$, the compact invariant set $M_0 = \{(\boldsymbol{x},\varphi,\boldsymbol{v}) : \boldsymbol{v} = \boldsymbol{u}(\boldsymbol{x},\varphi),\ \boldsymbol{x} \in D,\ \varphi \in [t_0-T, t_0+T]\}$ is completely filled with fixed points of (4). Note that M_0 is a graph over the compact domain $D_0 = \{(x,\varphi) : x \in D,\ \varphi \in [t_0-T, t_0+T]\}$; we show the geometry of D_0 and M_0 in Fig. 1a.

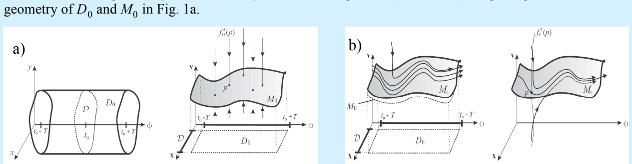

Fig 1: a) The geometry of the domain and the attracting set of fixed points M_0 ; each point p in M_0 has a two-dimensional stable manifold (unperturbed stable fiber at p) satisfying $(\boldsymbol{x}, \varphi)$ = const. b) The geometry of the slow manifold M_ε ; A trajectory intersecting a stable fiber converges to the trajectory through the fiber base point p.

Inspecting the Jacobian $d_v\left(\boldsymbol{u}(\boldsymbol{x},\varphi) - \boldsymbol{v}\right)\big|_{M_0} = -I_{n\times n}$ we find that M_0 attracts nearby trajectories at a uniform exponential rate of $exp(-\tau)$ (i.e., $exp(-t/\varepsilon)$ in terms of the original unscaled time). In fact, M_0 attracts all the solutions of (3) that satisfy $(\boldsymbol{x}(0),\varphi(0)) \in D\times[t_0-T, t_0+T]$; this can be verified using the last equation of (4) which is explicitly solvable for any constant value of $\boldsymbol{x}$ and φ. Consequently, M_0 is a compact normally hyperbolic invariant set that has an open domain of attraction. Note that M_0 is not a manifold because its boundary

$$\partial M_0 = \partial D \times [t_0 - T, t_0 + T] \bigcup D \times \{t_0 - T\} \bigcup D \times \{t_0 + T\}$$

has corners; $M_0 - \partial M_0$, however, is an $(n+1)$ – dimensional normally hyperbolic invariant manifold. By the results of Fenichel (Fenichel, 1979) for autonomous system any compact normally hyperbolic set of fixed points on gives rise to a nearby locally invariant manifold for system (3). (Local invariance means that trajectories can only leave the manifold through its boundary.) In our context, Fenichel's results guarantee the existence of $\varepsilon_0(t_0,T) > 0$, such that for all $\varepsilon \in [0, \varepsilon_0)$, system (4) admits an attracting locally invariant manifold M_ε that is $O(\varepsilon)$ C^r – close to M_0 (See Fig. 1b). By expanding the manifold M_ε into a Taylor series we have the following

***Theorem 1 (Haller & Sapsis, 2008)**: For small $\varepsilon > 0$ the equations of particle motion on the slow manifold can be written as*

$$\dot{\boldsymbol{x}} = \boldsymbol{u}_\varepsilon(t, \boldsymbol{x}) \equiv \boldsymbol{u}(t, \boldsymbol{x}) + \varepsilon \boldsymbol{u}^1(t, \boldsymbol{x}) + \varepsilon^2 \boldsymbol{u}^2(t, \boldsymbol{x}) + \ldots + \varepsilon^r \boldsymbol{u}^r(t, \boldsymbol{x}) + O\left(\varepsilon^{r+1}\right) \qquad (5)$$

where r is an arbitrary but finite integer, and the functions $\boldsymbol{u}^i(t, \boldsymbol{x})$ are given by

$$\begin{aligned} \boldsymbol{u}^1(t, \boldsymbol{x}) &= \left(\frac{3R}{2} - 1\right)\left(\frac{D\boldsymbol{u}}{Dt} - \boldsymbol{g}\right) \\ \boldsymbol{u}^k(t, \boldsymbol{x}) &= -\left[\frac{D\boldsymbol{u}^{k-1}}{Dt} + (\nabla \boldsymbol{u})\boldsymbol{u}^{k-1} + \sum_{i=1}^{k-2} (\nabla \boldsymbol{u}^i)\boldsymbol{u}^{k-i-1}\right] \quad k \geq 2. \end{aligned} \qquad (6)$$

We shall refer to (5) with the $\boldsymbol{u}^i(t, \boldsymbol{x})$ defined in (6) as the *inertial equation* associated with the fluid velocity field because (6) gives the general asymptotic form of inertial particle motion induced by $\boldsymbol{u}(t, \boldsymbol{x})$. A leading-order approximation to the inertial equations is given by

$$\dot{\boldsymbol{x}} = \boldsymbol{u}(t, \boldsymbol{x}) + \varepsilon\left(\frac{3R}{2} - 1\right)\left(\frac{D\boldsymbol{u}}{Dt} - g\right) + O\left(\varepsilon^2\right)$$

this is the lowest-order truncation of (5) that has nonzero divergence, and hence is capable of capturing clustering or dispersion arising from finite-size effects. The above argument renders the slow manifold M_ε over the fixed time interval $[t_0 - T, t_0 + T]$. Since the choice of t_0 and T was arbitrary, we can extend the existence result of M_ε to an arbitrary long finite time interval. Slow manifolds are typically not unique, but obey the same asymptotic expansion (5). Consequently, any two slow manifolds and the corresponding inertial equations are $O(\varepsilon^r)$ close to each other. Specifically, if $r = \infty$, then the difference between any two slow manifolds is exponentially small in ε. The case of neutrally buoyant particles ($R = 2/3$) turns out to be special: the slow manifold is the unique invariant surface $M_\varepsilon = \{(\boldsymbol{x},\varphi,\boldsymbol{v}) : \boldsymbol{v} = \boldsymbol{u}(\boldsymbol{x},\varphi),\ (\boldsymbol{x},\varphi) \in D_0\}$, on which the dynamics coincides with those of infinitesimally small particles. This invariant surface survives for arbitrary $\varepsilon > 0$, as noticed by Babiano et al. but may lose its stability for larger values of ε.

Global attractivity and local instabilities of the slow manifold

The above Theorem 1 seem to imply that inertial particles should synchronize exponentially fast with the inertial equation dynamics for small Stokes numbers. However, Babiano et al. and Vilela et al. give numerical evidence that two-dimensional suspensions do not approach Lagrangian particle motions; instead, their trajectories scatter

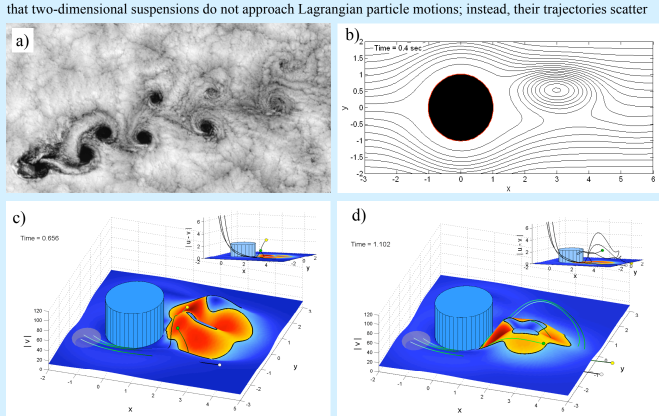

Fig 2: a) von Karman vortices in the atmosphere. b) Streamfunction simulating the von Karman vortices. c, d) Inertial particles in the von Karman velocity field. The colored surface represents the slow manifold that attracts trajectories over blue regions and repels them over red ones. The trajectories are computed using the full dynamical equations. Upper right plots show directly the distance from the manifold.

around unstable manifolds of the Lagrangian particle dynamics. Babiano et al. derive a criterion that characterizes the unstable regions in which scattering of inertial particles occurs. Their derivation follows an Okubo-Weiss-type heuristic reasoning, where it is assumed that the rate of change of the velocity gradient tensor calculated on a particle trajectory is small and hence can be neglected. However, as known counterexamples show (cf. Pierrehumbert and Yang) such reasoning, in general, yields incorrect stability results except near fixed points of the flow field.

In the following Theorem, we provide a rigorous analytical criterion for the stable and unstable regions of the slow manifold for weakly inertial particles in general three-dimensional unsteady fluid flows.

***Theorem 2 (Sapsis & Haller, 2008)**: For small $\varepsilon > 0$ the slow manifold is globally attractive if for all $\boldsymbol{x} \in D$*

$$\lambda_{\max}\left(-\frac{\nabla \boldsymbol{u}_\varepsilon(t, \boldsymbol{x}) + \left[\nabla \boldsymbol{u}_\varepsilon(t, \boldsymbol{x})\right]^T}{2}\right) < \frac{1}{\varepsilon} \qquad (7)$$

where $\lambda_{\max}$ denotes the maximum eigenvalue. Additionally, for any $\varepsilon > 0$ and $\boldsymbol{x} \in D$ such that condition (7) is violated the slow manifold M_ε repels all close enough trajectories $(\boldsymbol{x}(t), \boldsymbol{v}(t))$.

Application I : Inertial particles in the 2D von Karman vortex street in the wake of a cylinder

As a first application we consider inertial particle motion in the 2D von Karman vortex street model of Jung, Tel and Ziemniak (Fig. 2b). In Fig. 2c,d the slow manifold is presented as a surface colored according to the stability criterion (7). Specifically, red regions corresponds to spatial locations where dynamical instabilities will occur and hence particles' velocity will diverge from the velocity imposed by the inertial equation (5). In the upper right subplots (Fig. 2c,d) the distance from the slow manifold is presented directly in to illustrate more clearly the stability/instability regions of the slow manifold.

Application II : Inertial particles in hurricane Isabel (US East Coast, 2003)

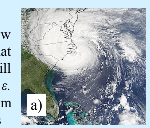

Our focus here is to study the dynamics of dust and droplet in the three-dimensional flow field of hurricane Isabel (cf. Fig. 3a) and locate the key three-dimensional structures that govern their motion. In Fig. 3b we present the regions where dynamical instabilities will take place according to criterion (7) for two different values of the inertial parameter ε. Fig. 3c show the attracting inertial Lagrangian coherent structures (ILCS) extracted from the backward Direct Lyapunov Exponent (DLE) field. In Fig 3d we shows all the points with DLE value greater than 80% of the maximum DLE value. Both plots refer to the case where the slow manifold is globally stable so we have rapid alignment of inertial particles with the ILCS. This is not the case for Fig 3e where the inertia parameter is larger and the ILCS derived from the inertial equation are not globally valid (red regions). Finally, in Fig 3f we superimpose both attracting and repelling ILCS (computed through the inertial equation) colored according to criterion (7) (yellow & red regions are unstable according to (7)).

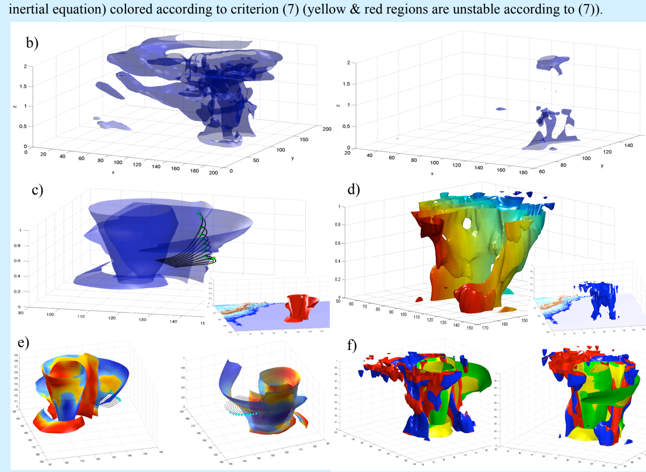

Fig 3: a) Satellite image of hurricane Isabel. b) Instability regions of the slow manifold according to criterion (7) for ε = 0.2 and ε = 0.1. c-d) Attracting and repelling ILCS for ε = 0.1. e) Attracting ILCS colored according to (7) for ε = 0.2. f) Attracting and repelling ILCS for ε = 0.2 colored according to (7) [yellow and red regions indicate locations where divergence of velocity from the slow manifold will occur].

Acknowledgments

This research was supported by NSF Grant DMS-04-04845, AFOSR Grant AFOSR FA 9550-06-0092, and a George and Marie Vergottis Fellowship at MIT. Hurricane Isabel data produced by the Weather Research and Forecast (WRF) model, courtesy of NCAR, and the U.S. National Science Foundation (NSF).

References

Babiano, A., Cartwright, J. H. E., Piro, O., and Provenzale, A., Dynamics of a small neutrally buoyant sphere in a fluid and targeting in Hamiltonian systems. *Phys. Rev. Lett*, **84** (2000) 5764-5767.

Fenichel, N., Geometric singular perturbation theory for ordinary differential equations. *J. Diff. Eqs.* **31** (1979) 51-98.

Haller G. and Sapsis T. , 'Where do inertial particles go in fluid flows?', *Physica D*, **237** (2008) 573-583.

R. T. Pierrehumbert, and H. Yang, "Global chaotic mixing on isentropic surfaces", *J. Atmos. Sci.* **50** 2462 (1993).

Sapsis, T., and Haller, G., Instabilities in the dynamics of neutrally buoyant particles, *Phys. Fluids*, **20**, (2008) 017102.

Sapsis, T., and Haller, G., Inertial particles dynamics in a hurricane, *(submitted)*

Vilela, R. D., de Moura, A. P. S., and Grebogi, C., Finite-size effects on open chaotic advection, *Phys. Rev. E* **73** (2006) 026302.